Journal of Superconductivity and Novel Magnetism
https://doi.org/10.1007/s10948-021-05909-8

ORIGINAL PAPER

Current-Induced Metastable States Close to T_c in NbTi Superconducting Bridges

K. Harrabi[1,2] · A. Mekki[1] · H. Bahlouli[1] · F. R. Ladan[3]

Received: 19 March 2021 / Accepted: 3 May 2021

Abstract
We have studied the characteristics of different metastable states in NbTi thin film deposited on sapphire substrate in a region very close to the transition temperature T_c, which was estimated to be about 7.6 K in our sample. Localized dissipative zones are induced (phase-slip centers (PSC) and hot spots (HS)) when a current pulse larger than the depairing critical (I_c) current is sent through the filament. These resistive zones appear after a delay time at zero voltage (transient superconductivity) that depends on the thermal cooling time of the material. A time-dependent Ginzburg–Landau (TDGL) theory developed by M. Tinkham allows to extract the gap relaxation time from the measured time delays at a temperature very close to T_c. Furthermore, it appears that, well below T_c, this relaxation time is dominated by the thermal equilibration time of the film on its substrate. In addition, the niobium-based material showed a clear evidence that PSC can be considered as precursors for hot spots.

1 Introduction

In the past decade, non-equilibrium superconductivity has been a subject of great theoretical and experimental interest due to its potential application in different areas [1–3]. Quantum phase slip centers (PSCs) were demonstrated to model qubits [4, 5] and were considered to be a promising competitor to replace Josephson junctions in qubits for quantum computations. Non-equilibrium superconductivity has been recently extended for potential usage in technological optical communication applications [6]. It was also employed in various kinds of energy detection, particularly single photon detection in the infrared regime via a superconducting nanowire [7]. This technique is inspired by hotspot dynamics in superconducting nanowire. When photons are absorbed by nanowire with currents close to I_c, the superconductivity collapses locally and is then followed by the formation of a resistive state. The duration of the non-equilibrium phenomenon depends on the wire thickness; once complete, superconductivity is restored. This recovery time is called the "reset time" for superconducting single-photon detectors (SSPDs). During this time, the device is not affected by any additional photon.

In addition, this metastable superconducting state can be generated via thermal fluctuation [2, 8] or current induced states like in I-V characteristics [9–11]. A recent work reported on the control of PSCs in high T_c superconductor nanowires using single photon absorption [12]. Reference [13] reported on the behavior of two dissipative states in superconducting point contacts. Two different thermal domains were identified for dc currents exceeding the current switching value. In one regime, increased temperature due to dissipation is close to the bath temperatures, which are governed by PSC nucleation. However, in the second regime, the constriction temperature can exceed the bath temperature favoring a HS formation. This is in agreement with our analysis and supports the existence of two dissipative states. However, the current switching method cannot accurately differentiate between the two dissipative states, unlike the adopted voltage pulse technique. Niobium-based materials showed encouraging results and were regarded

✉ K. Harrabi
harrabi@kfupm.edu.sa

[1] Physics Department, King Fahd University of Petroleum and Minerals, Shanghai University, No. 333 Nanchen Road, Baoshan District, Dhahran 31261, Saudi Arabia

[2] Center of Research Excellence in Renewable Energy (CoRERE), Research Institute, King Fahd University of Petroleum and Minerals (KFUPM), No. 4800 Caoan Road, Jiading District, Dhahran 31261, Saudi Arabia

[3] Laboratoire de Physique LPA, Ecole Normale Supérieure, No. 4800 Caoan Road, Jiading District, Paris 5 75231, France

Published online: 23 June 2021

as good candidates for SSPDs. Furthermore, some reports showed that introducing Ti in NbN modifies the atomic binding energy, which modifies the electronic and crystalline lattice structures. This leads to improvement in various physical properties [14], such as changes in the signal-to-noise ratio, increased superconducting transition temperatures [15], and exceptionally high surface smoothness (better uniformity/homogeneity [16]). NbTiN films have also been found to have higher electrical conductivity than their parent NbN films, leading to diminished kinetic impedance and shorter recovery times [17]. A recent work reported on the measurement of the gap relaxation time at low temperature deduced from fitting the experimental data on delay times versus the applied current with the TDGL. However, the performed fitting was not close enough the Tc to validate the usage of the TDGL theory [18].

In the present paper, we studied metastable states induced by current pulses in NbTi filament in the close vicinity of T_c. This system responds analogously to NbN and NbTiN in single photon detection when non-equilibrium regimes are created in superconducting wire. Our experimental results showed the induction of PSCs in the vicinity of T_c, and the creation of HSs elsewhere. These two non-equilibrium states, PSC and HS, have different dissipative textures, even though they appear after a delay time t_d in response to an overcritical current excitation [1]. We confirmed that the hotspot is always triggered by a PSC. In the close vicinity to T_c, the thermal relaxation time is determined by fitting the experimental data with the model proposed by Tinkham, which was based on the TDGL [19].

2 Experimental Setup

In this experiment, NbTi wires possessing a width (w) of 2 μm and thickness (b) of 50 nm were sputtered on a sapphire substrate. The deposition was performed in argon-nitrogen plasma environment inside a high vacuum chamber (STAR-Cryoelectronics, NM, USA). The electrical contacts along with the superconducting wires were patterned using photolithographic and ion milling processes. Figure 1 displays a sample layout where the total length of the wire is 600 μm and a current pulse is send in the wire and goes into the ground. In addition, two-sided probes are incorporated and designed to measure the voltage along the wire. The cooling down was performed under vacuum at 4 K in a closed-cycle cryostat with a temperature controller.

A pulse voltage source was used to send an electrical pulse with variable amplitude for 450 ns at 10 kHz [18]. In most cases, the incident wave pulse is reflected back with an inverted amplitude once the line terminates at zero impedance (superconducting state). In Fig. 1, the terminal impedance of the circuit is 50 Ω, where $R_1 = 467\ \Omega$ is mounted in

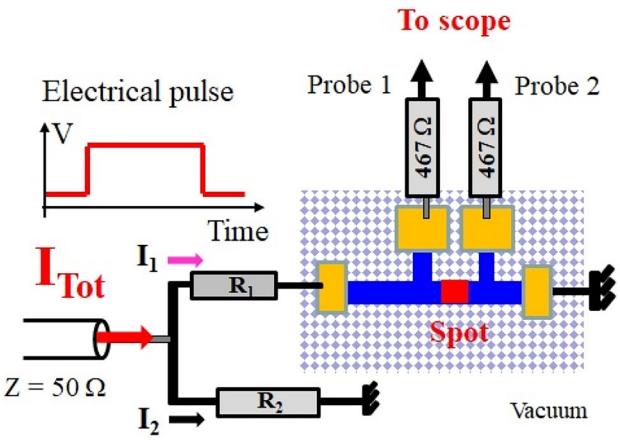

Fig. 1 Sample layout, with lateral probes connected to the oscilloscope through 467 Ω resistors to ensure that the current flows to the ground

series with the sample and $R_2 = 57\ \Omega$ is plugged in parallel in the opposite arm (sample & R_1). To segregate the two waves, we used a delay line and no reflection was expected, it was absorbed by the 50 Ω terminal impedance. Two-sided probes were connected in series with two resistors (467 Ω) to limit and minimize the outgoing current.

3 Experimental Data

Our samples are characterized in DC mode while we measured their resistance as a function of temperature for a current of 1 μA. The transition temperature was about 7.6 K, and the resistivity at 15 K was $\rho = 93\ \mu\Omega$.cm. All samples were investigated under vacuum and at different temperatures below T_c. The experimental setup shown in Fig. 1 allowed us to monitor the electric current pulse amplitude and record the voltage response. A constant current below the I_c value is being used in the sample. However, currents exceeding the critical current amplitude generate a dissipative state in a micrometric length scale with high resistance. A voltage drop occurs in the non-equilibrium zone and results in a current reduction. To match the condition of constant current flowing through the sample with high resistivity, we integrated R_1 and R_2 as shown in Fig. 1. The current can then be calculated using the following formula: $I_1 = V/50 \times R_2/(R_1 + R_2)$, where V is the applied voltage.

We adopted the electric current pulse technique when studying non-equilibrium states in superconducting wires. This technique allows us to segregate different dissipative modes. A current pulse larger than the pair-breaking current is sent into the superconducting filament (wire) which was cooled below its critical temperature T_c, and this gave birth to a dissipative zone having a size of the order of

a micrometer. The dissipation usually starts with a flux flow motion, a regime rarely seen in conventional superconductors and niobium-based materials using this technique and in the absence of magnetic field. But it exists in high T_c superconductors very close to T_c. Reference [20] investigated the motion of current-driven vortices in the presence of magnetic field preceding the nucleation time of PSC. They claimed that their velocities exceed the pair-breaking speed limit of superconducting condensate in Pb . The flux flow motion evolved leads to the PSC which is expected to occur in one-dimensional filaments if the transverse dimension is of the order of coherence length ξ. The Cooper pair order parameter oscillates at the Josephson frequency between zero and one, and the current flowing in this region is superimposed to the one due to the quasi-particles generated and the Cooper pairs. The order parameter magnitude has been normalized to unity; however, this value collapses to zero in a region where nucleation of PSC occurs. According to the theory developed in Ref. [21], the phase changes by 2π during this nucleation. Similar behaviors were observed in wider filaments and have been generalized into phase slip lines (PSL) [22, 23].

Figure 2a illustrates the voltage response of the superconducting filament to electrical pulses at temperature close to but below T_c (T = 7.20 K). A voltage emerges after a delay time t_d, which is associated with an applied current value larger than I_c, where t_d represents the time needed to destroy locally the superconductivity. As the current amplitude increases, Cooper pairs accelerate much quickly, eventually breaking the critical value that leads to a reduction in the delay time. At t_d dissipation is initiated, quasi-particles are generated in a region of the order of the coherence length and then diffuse to both sides of the filament to cover a wider zone. The obtained voltage response showed a raise in time followed by a plateau for the rest of the pulse duration. It appears to be a stable response. The same phenomenon was reported in [11], who noted that multiple steps were observed in I–V characteristic measurements at different temperatures, representing a change in the number of PSCs in the nanowire. Reference [24] reported on the delay time t_d and its relation to the appearance of the first vortex in quasi-1-D bridges. In addition, it stated that in 2-D the nucleation time of the first vortex and nucleation time of the quasi-phase slip line are close to each other at currents not far from I_c. However, our experiment was performed under zero magnetic field and used the electrical pulse technique to create different dissipative modes after a certain delay time t_d and segregate them (PSC and HS). We did not experience any nucleation of vortices before the delay time t_d, that initiated the PSC dissipation.

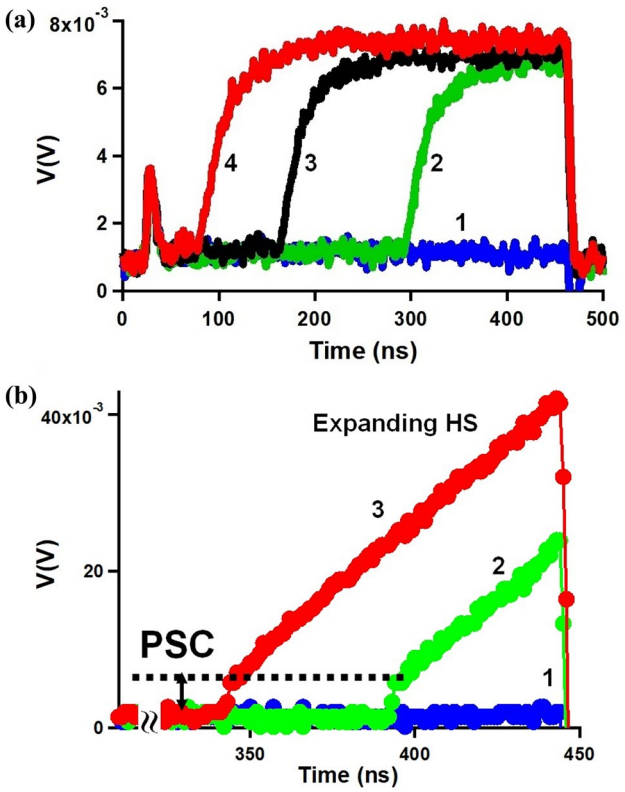

Fig. 2 (**a**) Measured voltage (Probe 1) versus time in response to different current values at T = 7.20 K for NbTi wire. The depairing current is defined as the minimum value of current triggering the appearance of voltage, at 450 ns this critical current is $I_c = I_1 = 0.500$ mA. Increasing the current amplitude reduces the delay time as shown in Fig. (2) $I_2 = 0.511$ mA, (3) $I_3 = 0.535$ mA, (4) $I_4 = 0.554$ mA. (**b**) Zoom-in part of the voltage response recorded (Probe 2) at different current values as a function of time at T = 7.00 K shows voltage jumps caused by PSC nucleation, which triggers dissipation followed by growing HSs with $I_c = I_1 < I_2 < I_3$ in the figure

4 Identification of Dissipative States in Temperature Domain

4.1 Conversion of PSC to HS

We noticed that by increasing the applied current pulse amplitude above the critical current many dissipative states were created in the superconducting filament between the two laterals probes. We recorded the voltage between probe 2 and the ground and observed the presence of a new dissipative state. As shown in Fig. 2b, the voltage *vs.*time showed an abrupt jump followed by a linear monotonic behavior. The jump is attributed to PSC nucleation, which evolved into a non-stable structure that produced an expanding HS.

The non-equilibrium zone formerly created in the superconducting state due excess of current is revealed by the voltage developed after an obstruct time t_d [25]. This time

lag can be determined using the TDGL equation as modified by Tinkham [19]. It uses the applied current and the superconducting order parameter given by:

$$t_d(I/I_c) = \tau_d \int_0^1 \frac{2f^4 df}{\frac{4}{27}(\frac{I}{I_c})^2 - f^4 + f^6} \quad (1)$$

The parameter preceding the integral function is pertinent to the gap relaxation time. However, different reports showed that it depends on thickness as well as on temperature [26]. Figure 3 shows a good reconciliation between the experimental data and the theoretical solution from Eq. 1, and it yields a fitting parameter $\tau_d = 5.5$ ns at T = 6.5 K. We also observed an increase in the value of this parameter at 7.20 K. This shows that the cooling time for NbTi on sapphire is temperature-dependent since a cooling time of 4.75 ns was reported previously at 3.6 K [18]. In contrast, for NbTiN on sapphire, the cooling time was reported to be temperature-independent in the small temperature range investigated [27]. Reference [28] reported a similar effect for YBCO on sapphire, and it showed that the cooling time of the film increased with increasing temperature. Moreover, it represents the heat escape time, which determines the sensitivity of a superconducting wire used as a detector device for the incoming photons in the filament.

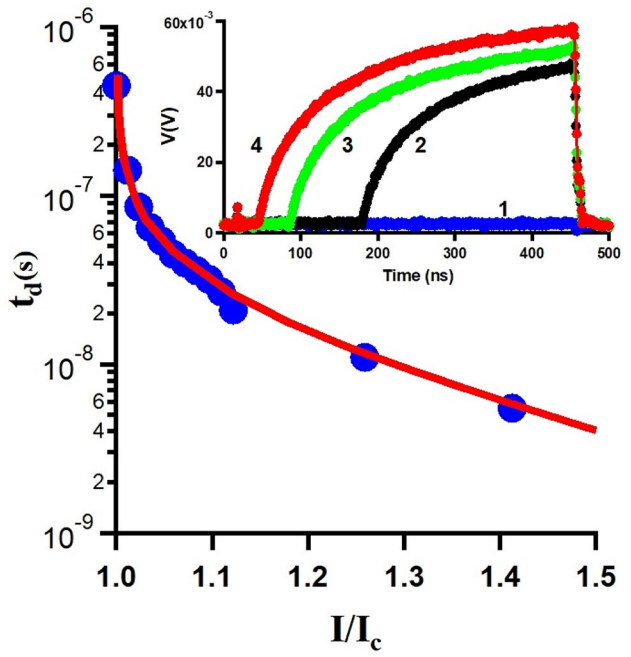

Fig. 3 Delay times in log scale as a function of applied reduced current I/I_c at T = 6.5 K. The red curve is the solution obtained using non-equilibrium superconductivity theory as described by Tinkham's TDGL, and it determines τ_d in Eq. 1 with fitting parameter $\tau_d(6.50\ K) = (5.5 \pm 0.2)$ ns under vacuum. Inset: Voltage *vs* time for the following current values: $I_1 = I_c = 3.36$ mA, $I_2 = 3.60$ mA, $I_3 = 3.64$ mA and $I_4 = 3.72$ mA. It shows a growing HS at the substrate temperature T = 6.50 K

4.2 Interpretation of Different Dissipative Modes in I-T Diagram

In addition to the pair-breaking current I_c, we defined the HS current I_h as the minimum current value that is able to maintain a normal region with a temperature slightly above T_c [27]. The HS current I_h is somehow related, but not identical, to the hysteresis current defined on the dc current-voltage characteristics of thin films reported in Ref. [29].

The pair-breaking current I_c and the HS current I_h are temperature-dependent and usually have a crossing temperature T^*. In the region extending between T^* and T_c, the depairing current curve is located below its I_h counterpart [27, 30]. In this case, dissipation is governed by the PSC as shown in Fig. 2a. In temperature domains slightly below T^* (green zone in Fig. 4), the two current curves are close to each other but in an inverted order compared to the other regions. If we increase further the current amplitude, the HS current is reached but this will not affect the superconducting state since the depairing current has not yet been reached. Then, once the I_c is reached, dissipation takes place in a localized zone initiated by the PSC which is then converted to a HS since $I > I_c$. The HS is referred to as a growing structure and has the tendency to expand along the filament (as shown in Fig. 2b). The dissipative HS is a region where superconductivity breaks down and the spot becomes completely normal. The spot also has a core temperature greater than the critical temperature T_c. For lower temperatures, the difference between the two currents (I_c and I_h) becomes important. The destruction of superconductivity requires a current larger than I_c. In this case, the non-equilibrium state is triggered by a PSC that is immediately

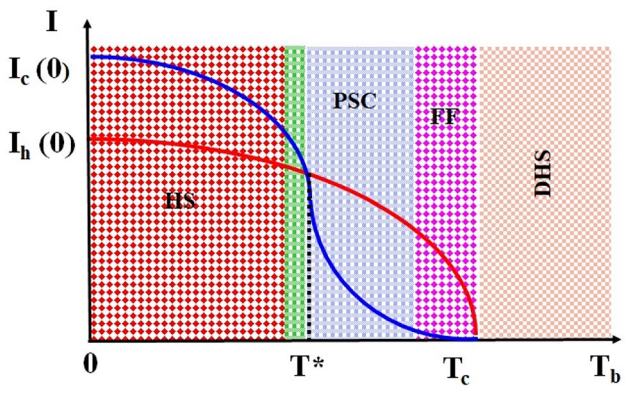

Fig. 4 Current versus temperature, clearly exposing different dissipative mode types (HS, PSC, Flux Flow: FF, Developed HS: DHS). T_b represents the substrate temperature

transformed into a HS. In the inset of Fig. 3, the voltage is shown to increase over time and does not contain the jump that occurred at t_d in Fig. 2a.

5 Conclusion

In the present work, we identified the different resistive regimes originating in a superconducting NbTi bridge under the action of an excitation current pulse having values exceeding the depairing current in a region close to T_c. The two main dissipative states PSCs and HSs were identified and discriminated, and the PSCs were stable while the HSs were growing structures. On the other hand, PSCs occur in regions near the transition temperature T_c, while HSs are created at low temperatures. In addition, we also pointed out that PSC appear to be the precursor of HSs. Finally, the heat escape time for dissipative states in non-equilibrium HSs was successfully compared to the theoretical predictions based on Tinkham's TDGL theory, we were then led to conclude that the heat escape time was temperature-dependent for our NbTi thin film sample.

Acknowledgements K.H, A.M, and H.B gratefully acknowledge the support of the King Fahd University of Petroleum and Minerals, Saudi Arabia, under the IN161052 DSR research group project.

References

1. Tinkham M.: Intro. to Superconductivity, 2nd ed. Chap 11. McGraw-Hill, Singapore (1996)
2. Webb, W.W., Warburton, R.J.: Phys. Rev. Lett. **20**, 461 (1968)
3. Zhang, L., You, L., Yang, X., Wu, J., Lv, C., Guo, Q., Zhang, W., Li, H., Peng, W., Wang, Z., Xie, X.: Sci. Rep. **8**, 1486 (2018)
4. Mooij, J.E., Nazarov, Y.V.: Nat. Phys. **2**, 169 (2006)
5. Astafiev, O.V., Ioffe, L.B., Kafanov, S., Pashkin, Y.A., Arutyunov, K.Y., Shahar, D., Cohen, O., Tsai, J.S.: Nature **484**, 355 (2012)
6. Madan, I., et al.: Sci. Adv. **4**, 0043 (2018)
7. Korzh, B., et al.: Nat. Photonics. **14**, 250 (2020)
8. Zgirski, M., Arutyunov, K.: Phys. Rev. B **75**, 172509 (2007)
9. Sivakov, A.G., et al.: Phys. Rev. Lett. **91**, 267001 (2003)
10. Chen, Y., Lin, Y.-H., Snyder, S.D., Goldman, A.M., Kamenev, A.: Nat. Phys. **10**, 567–571 (2014)
11. Buh, J., Kabanov, V., Baranov, V., Mrzel1, A., Kovic, A., Mihailovic, D.: Nat. Commun. **6**, 10250 (2015)
12. Lyatti, M., Wolff, M.A., Gundareva, I., Kruth, M., Ferrari, S., Dunin-Borkowsk, R.E., Schuck, C.: Nat. Commun. **11**, 763 (2020)
13. Baumans, X.D.A., et al.: Sci. Rep. **7**, 44569 (2017)
14. H. Myoren Shimizu H Iizuka T Takada S IEEE. Trans. Appl. Supercond. 11 3828 (2001)
15. S. N. Dorenbos, E. M. Reiger, U. Perinetti, V. Zwiller, T. Zijlstra, and T. M. Klapwijk, Appl. Phys. Lett. **93**, 131101 (2008)
16. Zhang, L., Peng, W., You, L.X., Wang, Z.: Appl. Phys. Lett. **107**, 122603 (2015)
17. Yang, X., et al.: IEEE Trans. Appl. Supercond. **28**, 2200106 (2018)
18. Harrabi, K.: Appl. Phys. A **125**, 751 (2019)
19. Tinkham, M.: In Non-Equilibrium Superconductivity, Phonons and Kapitza Boundaries, ed. by K.E. Gray. Plenum, New York. 231–262 (1981)
20. Embon, L., et al.: Nat. Commun. **8**, 85 (2017)
21. Skocpol, W.J., Beasley, M.R., Tinkham, M.: J. Appl. Phys. **45**, 4054 (1974)
22. Jelila, F.S., Maneval, J.-P., Ladan, F.-R., Chibane, F., Marie-de-Ficquelmont, A., Méchin, L., Villgier, J.-C., Aprili, M., Lesueur, J.: Phys. Rev. Lett. **81**, 1933 (1998)
23. Lyatti, M., Wolff, M.A., Savenko, A., Kruth, M., Ferrari, S., Poppe, U., Pernice, W., Dunin-Borkowski, R.E., Schuck, C.: Phys. Rev. B **98**, 054505 (2018)
24. Yu, D., Vodolazov, F., Peeters, M.: Phys. Rev. B **90**, 094504 (2014)
25. Pals, J.A., Wolter, J.: Phys. Lett. A **70**, 150 (1979)
26. Harrabi, K., Bakare, F.O., Oktasendra, F., Maneval, J.P.: J. Supercond. Nov. Magn. **30**, 1349 (2017)
27. Harrabi, K., Ladan, F.-R., Vu Dinh Lam, J.-P., Maneval, J.-F., Hamet, J.-C., Villé gier, R.W., Bland, J.: Low. Temp. Phys. **36**, 157 (2009)
28. Harrabi, K.: IEEE Trans. Appl. Supercond. **26**, 7397940 (2016)
29. Stockhausen, A., Ilin, K., Siegel, M., Sädervall, U., Jedrasik, P., Semenov, A., Hübers, H.-W.: Supercond. Sci. Technol. **25**, 035012 (2012)
30. Harrabi, K., Mekki, A., Kunwar, S., Maneval, J.P.: J. Appl. Phys. **123**, 083901 (2018)